Nuclear Instruments and Methods in Physics Research B 365 (2015) 3–7

Contents lists available at ScienceDirect

Nuclear Instruments and Methods in Physics Research B

journal homepage: www.elsevier.com/locate/nimb

Use of ion-assisted techniques for determining the structure of TiO_2 nanotubes

Renata P. Renz, André L.M. Vargas, Roberto Hübler *

Physics Faculty, Materials and Nanostructures Laboratory, Pontifical Catholic University of Rio Grande do Sul, Av. Ipiranga 6681, Porto Alegre, RS 90619-900, Brazil

ARTICLE INFO

Article history:
Received 1 October 2014
Received in revised form 29 May 2015
Accepted 15 July 2015
Available online 25 July 2015

Keywords:
Titanium dioxide nanotube
Electrochemical anodization
Rutherford backscattering spectrometry

ABSTRACT

In recent years, several researchers have reported obtaining titanium dioxide nanotubes presenting a variety of advanced and functional properties for high-performance applications, e.g., for solar and fuel cells, gas sensor, self-cleaning and biomedical devices. Electrochemical oxidation of titanium has been widely used as a method for fabrication of self-organized titanium oxide nanotubes (TiO_2 NTs), since it is a simple and inexpensive process, which allows a great control over the size and configuration of the formed structure. Normally, the morphological and structural characterizations are based on images from scanning or transmission electron microscopy. The use of characterization techniques assisted by energetic ion beams, such as RBS or MEIS, can simultaneously evaluate the composition and structural properties of the nanotubes. In this work, titanium oxide nanotubes were obtained by electrochemical oxidation of commercially pure titanium via constant-voltage experiments varying the growth time and the potential applied in order to access the formation dynamics of the NTs, including inner and outer diameters as function of the length, and the formation of the end lace type porous layer. The characterizations made by RBS were compared by analysis of top and cross-sectional FEG-SEM images demonstrating a good compromise between them.

1. Introduction

In recent years self-organized nanotubes films have received increasing attention from the scientific community and have emerged as strong candidates for applications in various fields of knowledge. Especially TiO_2 nanotubes formed from processes of electrolytic anodizing [1–4]. Due to the simplicity in controlling parameters in an electrolytic process, many studies have been developed in order to study the processes of nanotubes formation, mainly by varying concentrations of electrolyte solutions and basic parameters such as temperature, time of anodization and applied voltage [5–7]. Despite the type of desired application, the usage of electrolyte solutions formed by dissolving ammonium fluoride (NH_4F) in water and ethylene glycol (EG) has been virtually a consensus, due to its high viscosity, which generates a more accurate control and the formation of longer tubes [8,9]. These studies allowed us to evaluate the nanotubes formation process using a combination of analyzes of scanning electron microscopy (FEG-SEM) and transmission (X-TEM) showing important factors of the structure of these films. As examples we can list the change of the internal and external diameter as the tube length increases; the formation of the ribs on the nanotubes walls; the formation of oxide layers not arranged on surface of the tubes (non tubular disordered oxide layers, such as nanograss) and, in some cases, the formation of a porous covering lace type layer on the top surface of the self-organizing tubes [6,9,10]. Several authors have used, in addition to microscopy techniques, RBS analysis to show the effects of channeling in tubular layers, in order to evaluate the length of the tube by the decreasing of the apparent density of the metal plateau (titanium plateau in the case TiO_2 tubes) [7,11,12].

The theoretical explanation of the RBS technique is based on the probability of backscattered ions, eg, alpha particles on the surface of a sample. This backscatter depends mainly on the surface density of a given element and the scattering geometry. Which allows the evaluation of the atomic concentrations and depth profiles, experimentally [11–13] and comparing with simulation software, such as RUMP [14]. The RBS analyses of self-organizing nanotubes are made usually with incident alpha particles with energy between 1.5 and 5 MeV, allowing the visualization of the entire length of the tubes and differentiate them from the metal substrate. With such energy values, the interaction of alpha particles on the surface is very small due to the low stopping power,

* Corresponding author. Tel.: +55 5133537822.
E-mail address: hubler@pucrs.br (R. Hübler).

http://dx.doi.org/10.1016/j.nimb.2015.07.083
0168-583X/

preventing the observation of small density changes in this region, as the ones occurring in porous layers surfaces. To allow observation of these type of lace structures, formed on the surface, we chose to evaluate the films with an energy of one MeV, sacrificing the observation of the tube length, but allowing observing the variations in porosity and determine the structures of the films layers.

2. Materials and methods

In this work we used 0.65 mm thick commercially pure (ASTM grade 1) titanium plates (TiBrasil Titânio Ltda) to produce the TiO_2 nanotubes by sonoelectrochemical anodization. Prior to anodization, the titanium plates were mechanically polished and cleaned with acetone and deionized (DI) water for 15 min each in a 40 kHz ultrasound bath and then dried under N_2 flow. The electrochemical anodization was carried out in a conventional two-electrode system (Ti plate as the anode and the Pt sheet as the counter electrode, 10 mm separation) equipped with a direct current (DC) power supply. Ethylene glycol containing 0.5 wt% ammonium fluoride (NH_4F) and 10 vol% DI water was used as electrolyte. The anodization was conducted at 40 kHz sonication, in order to enhance the mobility of the ions inside the electrolyte. In order to minimize thermal effects during anodization, a mixture of water and ice at a constant temperature of 0 °C was used to conduct the mechanical waves in the ultrasonic bath. Fig. 1 shows a schematic diagram of the experimental apparatus. To produce TiO_2 NTs with different tube diameter and length, anodizations were performed at different voltages (from 10 V to 60 V applied onto the electrodes without ramping) for 30, 60 and 90 min. After anodization, the samples were rinsed with DI water followed by an ethanol bath for 15 min and then dried in air. All samples were produced in triplicate in order to minimize statistical errors. The structure and morphology of the TiO_2 nanotube films were characterized using a field-emission scanning electron microscope (FEG-SEM, FEI Inspect F50) and a transmission electron microscope (FEI Tecnai G2T20) using a top and cross-sectional view. The diameters of the nanotubes were obtained from the top-view FEG-SEM images by averaging the measures of the longitudinal and cross-sections of each tube, using a public domain image processing program (ImageJ, NIH, USA). The average value was calculated from at least 100 different measurements done on each sample's image. The RBS analyses were carried out in a 3MV Tanden ion implanter (IF-UFRGS) with a silicon barrier detector (15 keV) using alpha incidence normal to de surface. The particles were detected at two backscattering detectors positioned at + and −165° relative to the incidence beam. To optimize the energy resolution at the titanium backscattering energy, one detector was calibrated using a titanium pattern with backscattering edge at channel 400 allowing better observe the surface layers of the tubes but preventing observing heavy contaminants, and the other detector was calibrated using a gold pattern (Au edge at channel 400). All spectra were obtained using an EG&G multichannel with 512 channels and the data were fitted using the RUMP program [14].

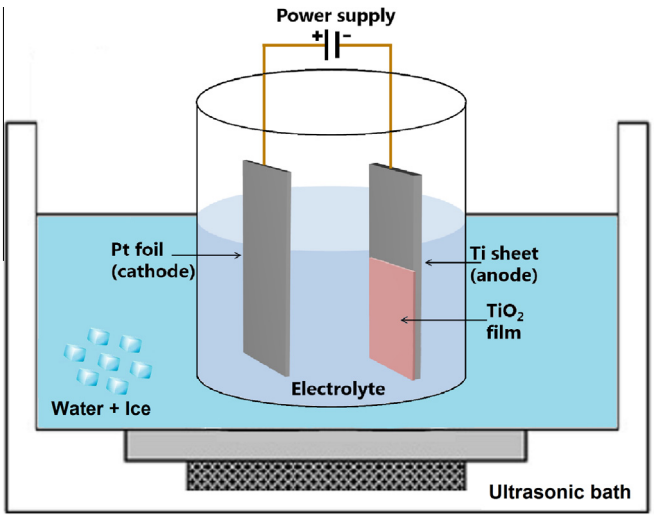

Fig. 1. Schematic diagram of the electrochemical cell used in the present work.

3. Results and discussion

3.1. Morphology of anodized films

The oxide layers obtained in this study showed a similar behavior to that observed in the literature for the tubes diameters. However, a diameter stabilization tendency was observed from a voltage of 50 V. Fig. 2a shows the average diameters of the tubes in which we may observe an almost linear behavior for voltages between 10 V and 40 V and a tendency to stabilize after 50 V, the same result was obtained by Macak et al. for a Ti–Nb alloy [15]. In the other hand, Ni and coauthors [8] obtained a linear behavior for the same electrolyte for potential between 120 and 220 V. Fig. 2b shows the length of the tubes as a function of the anodizing time for samples deposited at 20 V and 60 V which is possible to

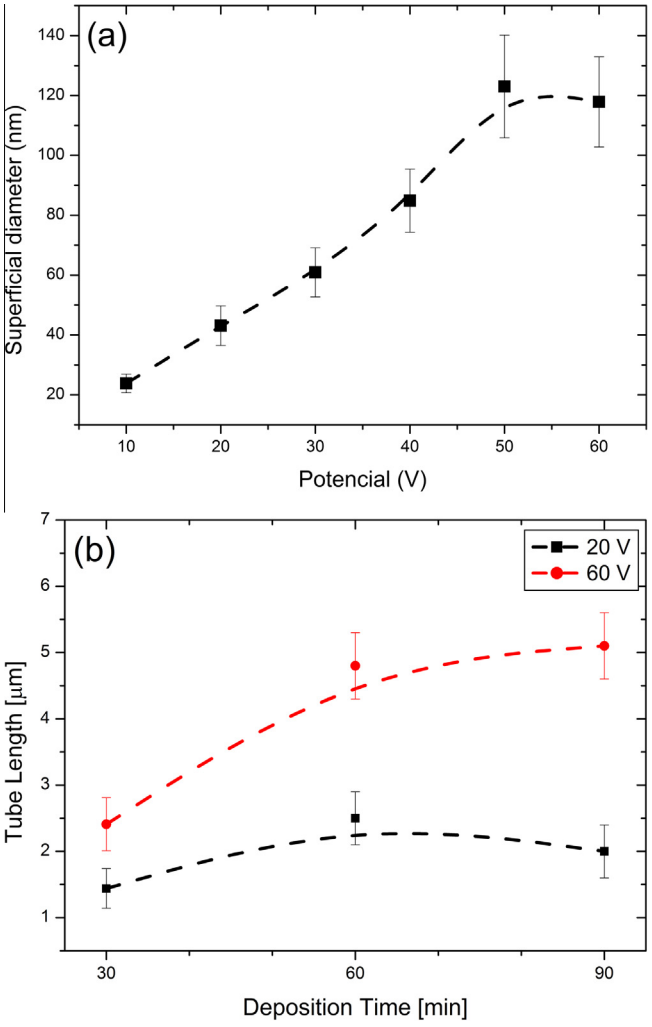

Fig. 2. Dependence of the (a) tube internal diameters and (b) nanotube length on the electrodes applied voltage.

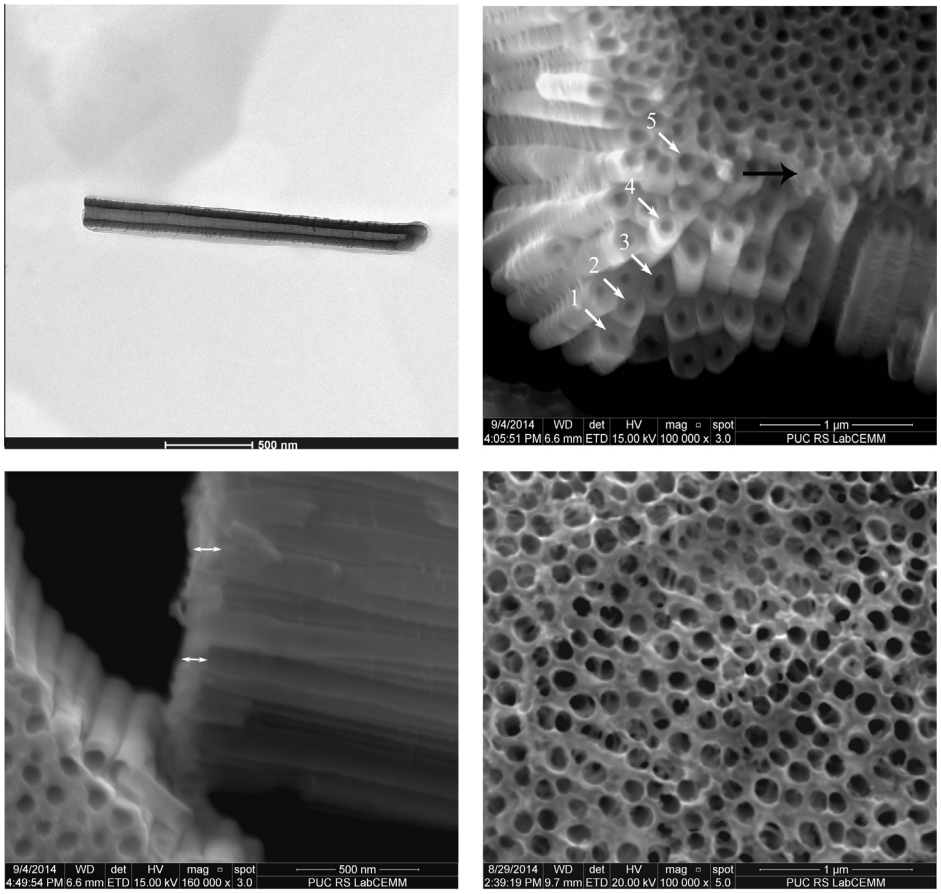

Fig. 3. Electron micrographs of the TiO_2 nanotubes. (a) Transmission view (X-TEM) of an isolated tube deposited at 40V – 60 min; (b) SEM of a fractured sample, where the white arrows – 1 to 5 – indicate the increase of internal diameter of the nanotubes along their lengths. The black arrow shows the formation of a discontinued porous oxide layer independent of the tubes; (c) cross-sectional image of the nanotubes where the white arrows indicate the porous oxide layer length, and (d) top view of the porous layer.

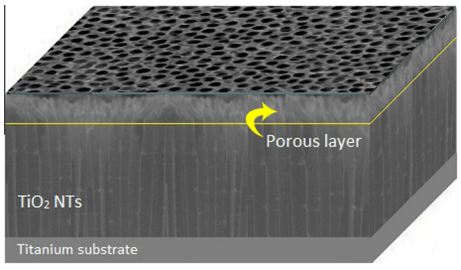

Fig. 4. Structural 3D model for the anodized titanium plate.

observe a trend to a length threshold for the tubes within this working procedure. This behavior may indicate that, under these deposition conditions, the competition between the growth of the tube and dissolution of the surface due to etching reached a dynamic equilibrium. Under these conditions the final length of the tubes only depends on the applied potential.

Fig. 3 shows the images of the tubes, allowing observing the dynamics of their formation. Fig. 3a shows a cross-sectional image of transmission electron microscopy (X-TEM) of an isolated nanotube (40 V – 60 min) where one can see that the inner diameter gradually increases from the base to the top of the tube surface. It can also be observed in Fig. 3b that the internal diameter of the nanotubes increases as the tubes grow, presenting a size gradient along their lengths (v-shape) indicated by indices 1–5, the white arrows in the figure. It is also possible to observe that there is a formation of a discontinued oxide layer independent from the tubes, indicated by the black arrow in the figure. These gradients are due to a chemical dissolution of TiO_2 occurring along the entire length of the tube, caused by the high concentration of fluoride ions in the electrolyte. The formation rate of the nanotubes and dissolution of the resulting oxide layer are determined by the composition of the electrolyte and the applied voltage. Thus, for samples under the same process conditions, due to the high concentrations of fluoride ions in the electrolyte, instead of obtaining longer tubes as a result of longer anodization, we will obtain tubes with thinner walls and bigger top diameter compared to its bases. In this way, the external walls also suffers an attack (very moderated) along its length, resulting in the thinning of the tube walls to the same extent that they grow, forming bonds between the small tubes (ribs). Various authors [5–10] present this behavior describing the formation of hexagonal structures connecting the tubes and Hsu et al. [10] shows the formation of a stable structure of nanowires as a result of the decomposition of the tubes after a certain time. Fig. 3c shows a cross-sectional image where we can clearly observe a structure of tubes with different density. Fig. 3d a top view of this porous layer where we can observe a low density lacey like structure, which allows the observation of end of the tubes below it. Assuming that the deposition system has reached equilibrium, where the growth rate of the films is equal to the removal rate of the oxide layer, which generates the porous layer, we have created a structural model for the anodized titanium substrates, as shown in Fig. 4.

3.2. Densities model for RBS analysis

Based on the data acquired from Fig. 4, it was possible to build a model describing the variation of porosity along the path of alpha

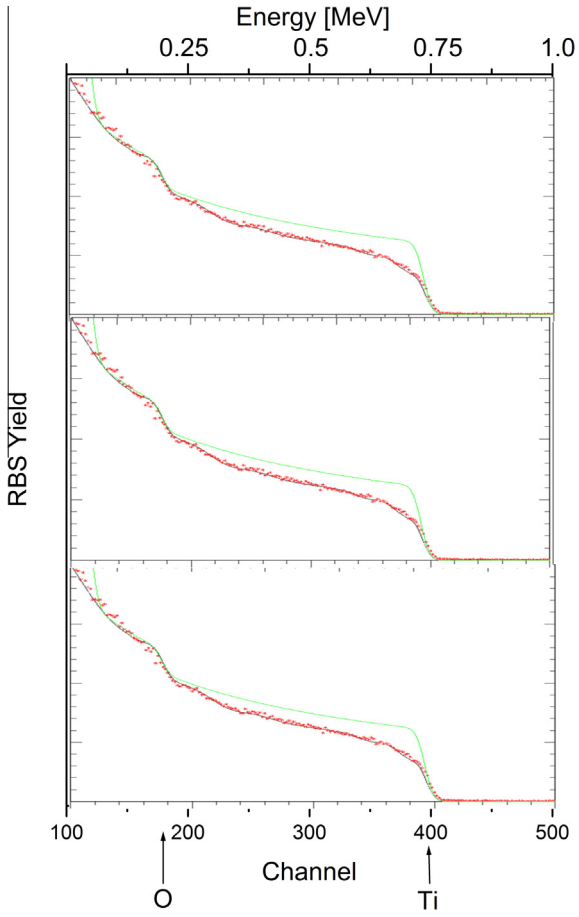

Fig. 5. RBS spectra for the samples anodized at 20 V, 40 V and 60 V, where the red dots represent the experimental data and the solid curves are the RUMP simulated spectra of the TiO_2-NTs (Black) and solid TiO_2 film (green). (For interpretation of the references to color in this figure legend, the reader is referred to the web version of this article.)

particles inside the film until reaching the titanium substrate. For this purpose, we propose a reduced density for the surface layer, representing the porous layer, followed by a thin layer of higher density, representing the interface between the porous layer and the TiO_2 nanotubes. A gradient of increasing density occurs along the length of the tubes of the films, corresponding to an increase in the wall thickness and consequent reduction of the internal diameter. To represent this change in the nanotube diameter in RUMP program, we include in the composition of TiO_2 sublayer a variable amount of hydrogen (increasing the hydrogen percentage whenever the diameter tube increases). This artifice allowed simulates the gradient channeling effect observed in the experimental data and evidence that the internal diameter of the tubes varies linearly from the base to the surface as seen in the X-TEM image (Fig. 3a and b). At the end of the formation process (Fig. 5 channel 200–210) a significant increase in the RBS Yield can be observed, corresponding to the end of the tube, followed by an elevated gradient until it reaches a concentration of titanium metal, corresponding to the unoxidized substrate. This proposal was simulated in the RUMP program keeping the O:Ti ratio equal to 2:1 throughout the length of the film, and the film porosity was simulated by including amounts of hydrogen in the sublayers composition. Thus the RUMP program calculates the new RBS Yield using the rule of mixtures including a hydrogen percentage in the layer which results in a reduction in the spectrum height. The concentrations of hydrogen (which are not detected in the RBS) will decrease as the inner diameter of the tube decreases until it reaches the simulated signal strength of a monolithic TiO_2 films.

Fig. 5 shows the RBS spectra for applied voltages of 20 V, 40 V and 60 V, where the dots represent the experimental data and the solid curve over the dots shows the approximation adjustment described previously. In addition, with the purpose of illustrate the density reduction of the titanium due to tube formation, a simulation of a dense film of TiO_2 is also displayed in the graphic. It is possible to observe a good correlation between experimental dots and the theoretical curve, which allows us to observe an apparent increase in the effect channeling as the applied voltage increases. In order to improve this measurement accuracy, we evaluated only the graphics with solid lines of the RUMP simulations for nanotubes and the TiO_2 dense film. Fig. 6a shows a comparison of the simulations of RBS for the 20 V, 40 V and 60 V samples, and Fig. 6b shows a zoom of the same simulation with emphasis on the surface of the films. This result allows us to observe that after a certain depth the behavior of the tube in relation to the RBS is equivalent to that found in the literature, corresponding to the spectra obtained from alpha particles with high energies. However, it can be observed in the most superficial part of the spectrum (E > 640 keV) significant differences related to the porous layers. It is possible to observe that the film deposited with a voltage of 40 V (which had cracks in the porous layer) has a smaller density than the film deposited at 60 V. In the inner layers, however, the effect of the larger diameter tube with low density prevails.

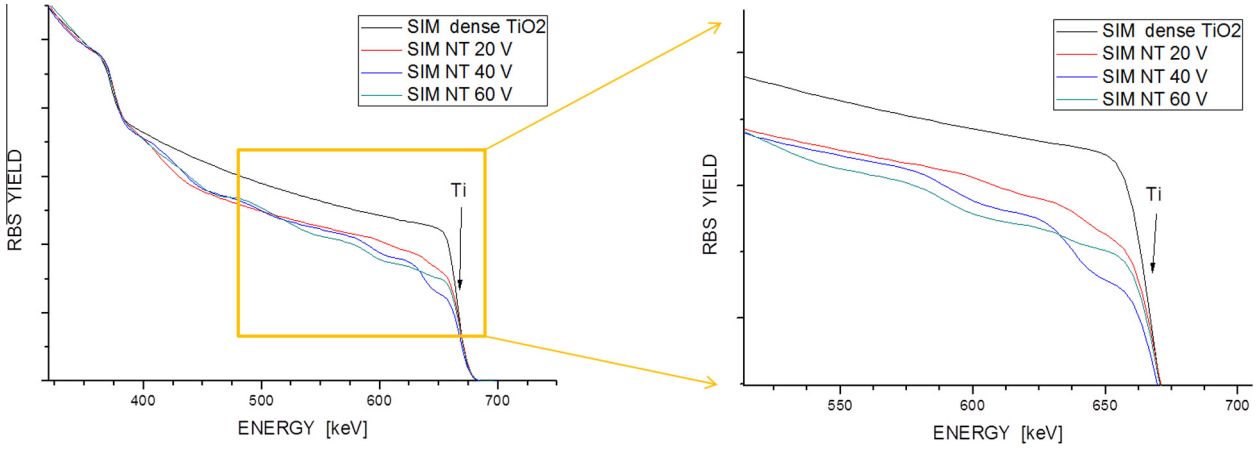

Fig. 6. (a) Comparison of the RBS simulations for the 20 V, 40 V and 60 V samples, and (b) a zoom of the same simulation with emphasis on the surface of the films.

4. Final considerations

For the experimental setup used in this research, we observed a linear growth behavior of the diameter of the tubes with the applied voltage, tending to a limit from 50 V. The length of the tubes does not follow a linear behavior with time of deposition. We observe that the attack of fluoride ions in the presence of water also exerts an attack at the top of the tubes, which ultimately decrease the internal and external wall thickness of the tubes.

The differential adjustment in the gain of the detectors allowed us to observe small changes in the films densities, allowing us to construct a theoretic model for the growing dynamics of these nanotubes. These analyzes would be impossible with the use of higher energies.

Acknowledgments

The authors gratefully acknowledge the assistance of Ion Implantation Laboratory of UFRGS for the RBS analysis, LabCEMM for the FEG images and Materials and Nanoscience Laboratory for the samples characterization and preparation. This work was financial supported by CAPES and CNPq, Brazilian research agencies.

References

[1] S. Bauer, A. Pittrof, H. Tsuchiya, P. Schmuki, Size-effects in TiO_2 nanotubes: diameter dependent anatase/rutile stabilization, Electrochem. Commun. 13 (2011) 538.
[2] J. Liu, M. Luo, Z. Yuan, A. Ping, Synthesis, characterization, and application of titanate nanotubes for Th(IV) adsorption, J. Radioanal. Nucl. Chem. 298 (2013) 1427.
[3] R. Camposeco, S. Castillo, I. Mejia, V. Mugica, R. Carrera, A. Montoya, M. M.-Pineda, J. Navarrete, R. Gómez, Active TiO_2 nanotubes for CO oxidation at low temperature, Catal. Commun. 17 (2012) 81.
[4] S.-In Na, S.-S. Kim, W.-K. Hong, J.-W. Park, J. Jo, Y.-C. Nah, T. Lee, D.-Y. Kim, Fabrication of TiO_2 nanotubes by using electrodeposited ZnO nanorod template and their application to hybrid solar cells, Electrochim. Acta 53 (2008) 2560.
[5] D. Regonini, A. Satka, A. Jaroenworaluck, D.W.E. Allsopp, C.R. Bowen, R. Stevens, Factors influencing surface morphology of anodized TiO_2 nanotubes, Electrochim. Acta 74 (2012) 244.
[6] Y.Q. Liang, Z.D. Cui, S.L. Zhu, X.J. Yang, Study on the formation micromechanism of TiO_2 nanotubes on pure titanium and the role of fluoride ions in electrolyte solutions, Thin Solid Films 519 (2011) 5150.
[7] A. Valota, D.J. LeClere, T. Hashimoto, P. Skeldon, G.E. Thompson, S. Berger, J. Kunze, P. Schmuki, The efficiency of nanotube formation on titanium anodized under voltage and current control in fluoride/glycerol electrolyte, Nanotechnology 19 (2008) 355701.
[8] J. Ni, K. Noh, C.J. Frandsen, S.D. Kong, G. He, T. Tang, S. Jin, Preparation of near micrometer-sized TiO_2 nanotube arrays by high voltage anodization, Mater. Sci. Eng., C 33 (2013) 259.
[9] A. Valota, D.J. LeClere, P. Skeldon, M. Curioni, T. Hashimoto, S. Berger, J. Kunze, P. Schmuki, G.E. Thompson, Influence of water content on nanotubular anodic titania formed in fluoride/glycerol electrolytes, Electrochim. Acta 54 (2009) 4321.
[10] Ming-Yi Hsu, Hsin-Ling Hsu, Jihperng Leu, TiO_2 nanowires on anodic TiO_2 nanotube arrays (TNWs/TNAs): formation mechanism and photocatalytic performance, J. Electrochem. Soc. 159 (8) (2012) H722.
[11] F. Muratore, A. Baron-Wiecheć, A. Gholinia, T. Hashimoto, P. Skeldon, G.E. Thompson, Comparison of nanotube formation on zirconium in fluoride/glycerol electrolytes at different anodizing potentials, Electrochim. Acta 58 (2011) 389.
[12] F. Muratore, T. Hashimoto, P. Skeldon, G.E. Thompson, Effect of ageing in the electrolyte and water on porous anodic films on zirconium, Corros. Sci. 53 (2011) 2299.
[13] E.K. Tentardini, C. Kwietniewski, F. Perini, E. Blando, R. Hübler, I.J.R. Baumvol, Deposition and characterization of non-isostructural $(Ti_{0.7}Al_{0.3}N)/(Ti_{0.3}Al_{0.7}N)$ multilayers, Surf. Coat. Technol. 203 (9) (2009) 1176.
[14] L.R. Doolittle, Algorithms for the rapid simulation of Rutherford backscattering spectra, Nucl. Instrum. Meth. Phys. Res. B (9) (1985) 344.
[15] J.M. Macak, H. Tsuchiya, A. Ghicov, K. Yasuda, R. Hahn, S. Bauer, P. Schmuki, TiO_2 nanotubes: self-organized electrochemical formation, properties and applications, Curr. Opin. Solid State Mater. Sci. 11 (2007) 3.